HHS Public Access

Author manuscript

Angew Chem Int Ed Engl. Author manuscript; available in PMC 2015 November 11.

Published in final edited form as:

Angew Chem Int Ed Engl. 2015 January 26; 54(5): 1461–1465. doi:10.1002/anie.201408529.

Targeted anti-thrombotic protein micelles

Wookhyun Kim[†], **Carolyn Haller**[†], **Erbin Dai**[†], **Xiowei Wang**[‡], **Christoph E. Hagemeyer**[‡], **David R. Liu**[#], **Karlheinz Peter**[‡], and **Elliot L. Chaikof**[†,*]

[†]Department of Surgery, Beth Israel Deaconess Medical Center, Harvard Medical School, and the Wyss Institute of Biologically Inspired Engineering of Harvard University, Boston, MA, USA

[‡]Atherothrombosis and Vascular Biology, Baker IDI Heart and Diabetes Institute, PO Box 6492, St Kilda Rd Central, Victoria 8008, Australia

[#]Howard Hughes Medical Institute, Department of Chemistry and Chemical Biology, Harvard University, Cambridge, Massachusetts 02138, USA

Abstract

Activated platelets provide a promising target for imaging inflammatory and thrombotic events along with site-specific delivery of a variety of therapeutic agents. Herein, we report the efficient design of multifunctional protein micelles bearing targeting and therapeutic proteins by one-pot transpeptidation using an evolved sortase A. Conjugation to the corona of a single-chain antibody (scFv), which binds to the ligand induced binding site (LIBS) of activated GPIIb/IIIa receptors enabled efficient detection of thrombi. Inhibiting thrombus formation was subsequently accomplished by incorporating the catalytically active domain of thrombomodulin (TM) onto the micelle corona for local generation of activated protein C, which serves to inhibit thrombin formation. An effective strategy has been developed for preparation of protein micelles that can be targeted to sites of activated platelets with broad potential for treatment of acute thrombotic events.

Platelets play a critical role in mediating thrombus formation with accumulating evidence demonstrating that platelets also participate in a wide range of inflammatory processes, which contribute to the development of atherosclerosis, cerebrovascular disease, rheumatoid arthritis, as well as inflammatory bowel disease, tumor growth and metastasis. Characteristically, the release of ADP, thrombin, thromboxane, and other pro-inflammatory factors at the sites of acute or chronic inflammation, regardless of etiology, can lead to activation of platelets and endothelial cells (ECs) with further recruitment of circulating platelets and inflammatory cells.[1] These cell-cell and cell-protein interactions are facilitated by various glycoproteins, including GPIbα, GPIIb/IIIa and P-selectin, abundantly expressed on the membrane surface of activated platelets. Considering the ubiquitous involvement of platelets in thrombosis and inflammation, a strategy targeting activated platelets provides a very attractive approach for the selective delivery of anti-thrombotic and anti-inflammatory agents. In particular, the glycoprotein IIb/IIIa (GPIIb/IIIa) undergoes a

*Address correspondence to: Elliot L. Chaikof, M.D., Ph.D., Department of Surgery, Beth Israel Deaconess Medical Center, 110 Francis St, Suite 9F, Boston, MA 02115, Tel: (617) 632-9581, echaikof@bidmc.harvard.edu.

conformational change at the time of platelet activation and, thereby, through the exposure of unique epitopes serves as a distinctive structural feature for selective targeting of activated platelets.[2] In this regard, single-chain antibodies have been developed that bind to the activated GPIIb/IIIa receptor with high affinity, such as a single-chain antibody (scFv) that binds to the ligand-induced binding site (LIBS) of GPIIb/IIIa (anti-LIBS scFv).[3]

Anti-thrombotic therapy is widely based on systemic drug delivery, which increases the risk of bleeding or other complications. To overcome these limitations, approaches for targeted delivery have been investigated.[4] For example, cyclic RGD-modified liposomes have been shown to display high affinity to activated platelets.[4c] It has also been demonstrated that conjugation of an anti-LIBS scFv to PEGylated microcapsules, iron oxide microparticles, or cells enabled targeted imaging to identify thrombi and platelet microaggregates associated with a variety of cardiovascular and inflammatory states.[4d, 4e] Anti-LIBS single-chain antibodies that contained diverse tagging motifs at the C-terminus were conjugated to microparticles through either non-covalent metal chelation or covalent chemoenzymatic conjugation methods. scFv-functionalized microparticles have shown highly specific binding to activated platelets with the capacity to image thrombi by magnetic resonance imaging (MRI) or ultrasound imaging.[5] Anti-LIBS-conjugated cells have also been targeted to activated platelets; suggesting the potential use of anti-LIBS scFv for targeted cell therapy.[4e]

Polymeric micelles are self-assembled nanoparticles with a core-shell structure and have recently emerged as a powerful therapeutic platform to detect and treat various disease states, especially cancer.[4f, 6] Advantages of polymeric micelles include their increased circulating half-life, high drug-loading capacity, and their ability to present multiple ligands for improved site-specific targeting. In this regard, block polypeptides, and in particular recombinant elastin-based protein polymers, represent a class of polymeric micelles that consist of chemically and conformationally distinct protein blocks self-assembled into a variety of diverse structures.[7] ELP protein micelles have several advantages over synthetic polymeric micelles in that they are biocompatible and biodegradable.[8] In addition, recombinant ELP block copolymers are highly monodisperse, which provides precise control over stereochemistry, amino acid sequence and molecular weight. Finally, the modular structure of ELP micelles is easily tailored and functionalized using either chemical or enzymatic methods. Diblock polypeptides fused to small proteins have afforded multivalent ELP micelles displaying proteins at the corona by temperature-mediated self assembly.[9] Tumor targeting has been pursued by genetically fusing RGD and NGR motifs to the hydrophilic portion of diblock ELPs.[10]

Herein, we describe the efficient and rapid formulation of multivalent, multifunctional protein micelles by one-pot transpeptidation using an evolved sortase A. Targeted delivery to activated platelets was achieved using a single-chain antibody that selectively binds to activated GPIIb/IIIa receptors.[4d, 4e, 11] In turn, thrombin generation was inhibited by incorporation of the catalytically active domain of thrombomodulin onto the micelle corona. Thrombomodulin alters the substrate specificity of thrombin, such that it preferentially activates Protein C, which subsequently inactivates coagulation Factors Va and VIIIa, thereby limiting further thrombin formation.[12] The effectiveness of this strategy in limiting

thrombus growth and propagation in vivo demonstrates the therapeutic potential of multifunctional protein micelles.

Although protein fusion can be readily achieved using recombinant DNA techniques, bacterial expression of a fusion construct may be limited by low yield, loss of protein activity due to protein misfolding, as well as the formation of inclusion bodies that require a refolding process.[13] As an alternative, chemical or enzymatic schemes can be used to mediate conjugation between reactive functional groups or appropriate peptide substrates. In this study, sortase-mediated bioconjugation was employed[4d, 4e, 14] to attach a single-chain antibody and a recombinant, catalytically active construct of thrombomodulin via C-terminal LPETG motifs to protein micelles bearing a N-terminal triglycine (GGG) oligopeptide. An amphiphilic diblock elastin-mimetic polypeptide was used to form spherical micelles (*d* ~50 nm), which self-assembled via a temperature-driven conformational change of the hydrophobic block.[7a] Diblocks were generated with a nucleophilic triglycine motif followed by a His tag that was genetically incorporated at the N-terminal end of hydrophilic block. The recombinant single-chain antibody selectively binds to activated GPIIb/IIIa receptors and was re-engineered with a C-terminal LPETG-His6 peptide motif. A human TM fragment containing the catalytically active EGF-like 456 domains was also expressed with a C-terminal LPETG motif (TM-LPETG), as well as an N-terminal FLAG-tag, which facilitated purification using anti-FLAG affinity chromatography.[15] An evolved sortase A pentamutant (eSrtA), previously generated by directed evolution,[16] was used to conjugate scFv, TM or both scFv and TM to the N-terminal GGG motif of the micelle corona so as to produce a set of multifunctional micelles (Scheme 1).

Protein conjugation to ELP micelles using eSrtA was first investigated by SDS-PAGE gel electrophoresis (Figure 1). Micelles were initially produced from an aqueous solution of GGG-diblock copolymer (8 μM) and then used in all reactions at a final concentration of 4 μM (CMC 3.5 μM). Micelles were incubated with LPETG-tagged scFv and eSrtA (1 μM) in a buffered solution (50 mM Tris-HCl, 150 mM NaCl, 0.5 mM $CaCl_2$, pH 7.5) at room temperature. Conjugation of scFv to the protein diblock afforded a scFv-LPET-GGG-diblock, as evident by a new band, which was 30 kD greater than the original diblock with maximum yield achieved in 1 hr (Figure 1A). Likewise, a TM-LPET-GGG-diblock conjugate was successfully obtained (Figure 1B). A low ratio of sortase to substrate was used to minimize side reactions, including the formation of acyl-enzyme intermediates and hydrolysis related side products. At a 1 μM concentration of eSrtA, functionalization of micelles with scFv (***scFv-micelle***) and TM (***TM-micelle***) was observed by 1 hr without side products. Reaction conditions were optimized for maximum conjugation of micelles with scFv or TM (Supp Info Figure S2 A, B). Incubation of GGG-micelle with scFv-LPETG (8 equivalents to GGG-diblock) or TM-LPETG (3 equivalents to GGG-diblock) afforded yields of approximately 15 and 50%, respectively, as quantified by SDS-PAGE gel analysis based on the ratio of GGG-diblock band intensity before and after conjugation. Diblock conjugates were not observed in the absence of eSrtA or in the presence of micelles that did not contain N-terminal GGG motifs (Figure 1A, B). Significant differences in the conjugation of scFv or TM was attributed to steric hindrance due to differences in protein size with less accessibility to the C-terminal LPETG motif of the scFv. Purification was

achieved by size-exclusion centrifugal filtration (MWCO 100 kDa) to remove unreacted LPETG-tagged scFv or TM and eSrtA.

DLS and TEM were used to characterize micelle conjugation (Figure 1C–E). Average diameters of scFv and TM micelles were 61 and 77 nm, respectively, which was larger than that of the initial GGG-micelle (50 nm), consistent with reports for TM-functionalized liposomes[17] and other protein-functionalized ELP micelles.[9a, 18] TEM demonstrated the formation of uniform spheres of 30 to 40 nm in diameter, consistent with imaging of micelles in a dehydrated state. The zeta potential of GGG-micelles, which contains glutamic acid residues in the outer shell was negative (−13 mV).[7d, 18] After conjugation with scFv or TM, the zeta potential at neutral pH decreased to −18 and −16 mV, respectively.

Binding of scFv-micelles to activated platelets was assessed by flow cytometry (Figure 1F,G). As anticipated, scFv-micelles did not bind to resting, non-activated platelets, but bound selectively to activated platelets, which was not observed for GGG-micelles. TM-micelle conjugation enhanced the production of activated Protein C (aPC) that was comparable to that of free TM-LPETG (Figure 1H). aPC was not generated by GGG-micelle in the absence of TM. These data indicate that scFv and TM remain fully active after conjugation to the hydrophilic shell of protein micelles.

Binding of micelles to platelet-rich thrombi was examined by intravital microscopy using a murine cremaster muscle microcirculation model in which thrombi were formed by laser-induced vascular injury. GGG- and scFv-targeted micelles containing N-terminal His-tags were pre-incubated with Alexa Fluor 488-conjugated to an anti-penta His antibody. Intravital microscopy demonstrated specific binding of targeted micelles to platelet-rich thrombi, whereas GGG-micelles displayed no detectable background binding (Figure 2).

The generation of multifunctional micelles requires the reliable introduction of multiple functional components.[4f, 4g, 6] Peters and colleagues have developed multifunctional micelles that target fibrin deposited on atherosclerotic plaques.[4f] Likewise, PEG-lipid micelles have been functionalized with a fibrin-targeting peptide (CREKA), a fluorescent dye, and hirulog, for targeted delivery of an anticoagulant to sites of atherosclerosis. Co-functionalization of nano/micro-particles or DNA scaffolds has been developed by physical adsorption, biotin-streptavidin interaction or chemical coupling techniques for application in biosensors, cofactor recycling or biocatalytic cascades for the synthesis of biological materials.[19] Although these techniques are simple, it is hard to achieve fully active proteins after functionalization because of the potential for non-specific conjugations or mis-orientation of proteins, leading to loss of protein activity. In this report, anti-LIBS scFv facilitated selective micelle binding to activated GPIIb/IIIa receptors, while TM enhanced thrombin-mediated aPC generation. Micelles were functionalized with both LPETG-tagged proteins using a one-pot sortase reaction scheme (Scheme 1C). Briefly, GGG-micelles were incubated with anti-LIBS scFv-LPETG and TM-LPETG in the presence of eSrtA (1 hr incubation, 4 μM GGG-diblock, 30 μM scFv-LPETG, 12 μM TM-LPETG, 1 μM eSrtA). Conjugation of scFv and TM to protein micelles produced two new bands on SDS PAGE gels corresponding to the scFv-LPET-GGG-diblock and TM-LPET-GGG-diblock (Figure 3A). Optimized reaction conditions allowed co-functionalization to GGG-diblocks within a

1 hr period using 8 equivalents of scFv-LPETG and 3 equivalents of TM-LPETG (Supp Info, Figure S2). Co-functionalization of micelles was confirmed by selective fluorescent labeling of TM, which afforded a single fluorescent band corresponding to the TM-LPET-GGG-diblock. The amount of conjugated TM was quantified via in-gel fluorescence scanning. Approximately 50% of the GGG-diblock was conjugated to TM (~10 μg of TM/100 μg of protein micelles) (Supp Info. Figure S3, S4).

The average diameter and zeta potential of bifunctional, scFv/TM-micelles (***targeted TM micelle***) were 75 nm and −14 mV, respectively (Figure 3B, C). TEM of dehydrated samples confirmed that these micelles were uniform spheres of 30 to 40 nm in diameter. Targeted TM micelles demonstrated specific binding to activated platelets by flow cytometry along with enhanced aPC generation, which was not observed using non-derivatized GGG-micelles (Figure 3 D, E). These results confirm that co-immobilization of scFv and TM afforded multivalent, multifunctional micelles that selectively bind to activated platelets with local generation of aPC.

The capacity of targeted TM-micelles to target and limit thrombus formation was investigated using intravital microscopy of localized laser-induced injury to murine cremaster arterioles (Figure 4).[20] Little change in platelet accumulation was observed after intravenous infusion of PBS, TM-micelles or scFv-micelles (Figure 4D). However, intravenous infusion of targeted TM-micelles lead to a significant reduction in platelet deposition despite local vessel wall injury. The approach described in this manuscript is motivated by the idea that clinical efficacy of anti-thrombotic therapy can be significantly improved through targeted delivery to sites of injury. The chosen targeting strategy is based upon the principle that activated platelets serve as an ideal epitope for the delivery of agents targeted to the site of vascular wall injury, given their early and spatial involvement in coagulation. To this end, we report site-specific modification of protein micelles with both a scFv targeting handle to activated platelets and an antithrombotic therapeutic handle. Through in vitro assays, we confirmed that both the scFv and the TM retain their individual function after conjugation to micelles. To examine the therapeutic significance of our targeting approach in vivo, we employed a well-established model of laser-injury induced arteriole thrombosis.[21] Intravital videomicroscopy allows real time monitoring of platelet accumulation as well as visualization of targeted micelles co-localizing with activated platelets. Significantly, we only observed enrichment of micelles that included scFv targeting functionalization (Figure 2) and we only observed inhibition of thrombus formation with micelles that included both scFv and TM (Figure 4). When equimolar dose of non-targeted TM-micelles were infused, there was no significant change in thrombus formation compared to saline controls and scFv-micelle controls. Thus, therapeutic targeting presents a promising approach to reduce elevated dosing strategies that are often required with systemic delivery.

In conclusion, we have developed multivalent, multifunctional protein micelles, functionalized with both a scFv specific to activated GPIIb/IIIa receptors and a human TM fragment using sortase-mediated bioconjugation. In comparison with previously reported studies that genetically fused small proteins (< 20 kDa) and peptides (3 – 20 amino acids) to micelle-forming ELP diblock polypeptides,[9a, 10a, 18] selective covalent conjugation of

multiple relatively large proteins (~ 40 kDa) was achieved without the loss of bioactivity. Chemoenzymatic bio-orthogonal conjugation provides a highly efficient strategy for co-functionalization of diverse molecules onto micelles or other nanoparticle carriers. In this study, multifunctional protein micelles displayed a high level of site-specific targeting to thrombi with local generation of an inhibitor of the coagulation cascade. These results prove the feasibility of targeted delivery of a potent anti-thrombotic to sites of platelet thrombi with a concomitant reduction in anticoagulant dose and bleeding risk.

Supplementary Material

Refer to Web version on PubMed Central for supplementary material.

References

1. a) Mackman N. Nature. 2008; 451:914–918. [PubMed: 18288180] b) Modery-Pawlowski CL, Kuo HH, Baldwin WM, Sen Gupta A. Nanomedicine (Lond). 2013; 8:1709–1727. [PubMed: 24074391] c) Rondina MT, Weyrich AS, Zimmerman GA. Circ Res. 2013; 112:1506–1519. [PubMed: 23704217]
2. Cox D, Brennan M, Moran N. Nat Rev Drug Discov. 2010; 9:804–820. [PubMed: 20885411]
3. a) Schwarz M, Rottgen P, Takada Y, Le Gall F, Knackmuss S, Bassler N, Buttner C, Little M, Bode C, Peter K. Faseb J. 2004; 18:1704–1706. [PubMed: 15522915] b) Hohmann JD, Wang X, Krajewski S, Selan C, Haller CA, Straub A, Chaikof EL, Nandurkar HH, Hagemeyer CE, Peter K. Blood. 2013; 121:3067–3075. [PubMed: 23380744]
4. a) Korin N, Kanapathipillai M, Matthews BD, Crescente M, Brill A, Mammoto T, Ghosh K, Jurek S, Bencherif SA, Bhatta D, Coskun AU, Feldman CL, Wagner DD, Ingber DE. Science. 2012; 337:738–742. [PubMed: 22767894] b) Wang Z, Li J, Cho J, Malik AB. Nat Nanotechnol. 2014; 9:204–210. [PubMed: 24561355] c) Huang G, Zhou Z, Srinivasan R, Penn MS, Kottke-Marchant K, Marchant RE, Gupta AS. Biomaterials. 2008; 29:1676–1685. [PubMed: 18192005] d) Leung MK, Hagemeyer CE, Johnston AP, Gonzales C, Kamphuis MM, Ardipradja K, Such GK, Peter K, Caruso F. Angew Chem Int Ed Engl. 2012; 51:7132–7136. [PubMed: 22744941] e) Ta HT, Prabhu S, Leitner E, Jia F, von Elverfeldt D, Jackson KE, Heidt T, Nair AK, Pearce H, von Zur Muhlen C, Wang X, Peter K, Hagemeyer CE. Circ Res. 2011; 109:365–373. [PubMed: 21700932] f) Peters D, Kastantin M, Kotamraju VR, Karmali PP, Gujraty K, Tirrell M, Ruoslahti E. Proc Natl Acad Sci U S A. 2009; 106:9815–9819. [PubMed: 19487682] g) Yurko VMY, Andreozzi E, Thompson GL, Vertegel AA. Mater Sci Eng, C. 2009; 29:737–741.
5. a) von zur Muhlen C, von Elverfeldt D, Moeller JA, Choudhury RP, Paul D, Hagemeyer CE, Olschewski M, Becker A, Neudorfer I, Bassler N, Schwarz M, Bode C, Peter K. Circulation. 2008; 118:258–267. [PubMed: 18574047] b) Wang X, Hagemeyer CE, Hohmann JD, Leitner E, Armstrong PC, Jia F, Olschewski M, Needles A, Peter K, Ahrens I. Circulation. 2012; 125:3117–3126. [PubMed: 22647975]
6. Shi J, Xiao Z, Kamaly N, Farokhzad OC. Acc Chem Res. 2011; 44:1123–1134. [PubMed: 21692448]
7. a) Kim W, Thevenot J, Ibarboure E, Lecommandoux S, Chaikof EL. Angew Chem Int Ed Engl. 2010; 49:4257–4260. [PubMed: 20446331] b) Dreher MR, Simnick AJ, Fischer K, Smith RJ, Patel A, Schmidt M, Chilkoti A. J Am Chem Soc. 2008; 130:687–694. [PubMed: 18085778] c) Kim W, Xiao J, Chaikof EL. Langmuir. 2011; 27:14329–14334. [PubMed: 21973265] d) Kim W, Brady C, Chaikof EL. Acta Biomater. 2012; 8:2476–2482. [PubMed: 22504077] e) Numata K, Kaplan DL. Adv Drug Deliv Rev. 2010; 62:1497–1508. [PubMed: 20298729]
8. a) Ong SR, Trabbic-Carlson KA, Nettles DL, Lim DW, Chilkoti A, Setton LA. Biomaterials. 2006; 27:1930–1935. [PubMed: 16278015] b) Shah M, Hsueh PY, Sun G, Chang HY, Janib SM, MacKay JA. Protein Sci. 2012; 21:743–750. [PubMed: 22434766]
9. a) Hassouneh W, Fischer K, MacEwan SR, Branscheid R, Fu CL, Liu R, Schmidt M, Chilkoti A. Biomacromolecules. 2012; 13:1598–1605. [PubMed: 22515311] b) Shi P, Aluri S, Lin YA, Shah

M, Edman M, Dhandhukia J, Cui H, MacKay JA. J Control Release. 2013; 171:330–338. [PubMed: 23714121] c) Sun G, Hsueh PY, Janib SM, Hamm-Alvarez S, MacKay JA. J Control Release. 2011; 155:218–226. [PubMed: 21699930]

10. a) Simnick AJ, Amiram M, Liu W, Hanna G, Dewhirst MW, Kontos CD, Chilkoti A. J Control Release. 2011; 155:144–151. [PubMed: 21763734] b) Simnick AJ, Valencia CA, Liu R, Chilkoti A. ACS Nano. 2010; 4:2217–2227. [PubMed: 20334355]
11. Schwarz M, Meade G, Stoll P, Ylanne J, Bassler N, Chen YC, Hagemeyer CE, Ahrens I, Moran N, Kenny D, Fitzgerald D, Bode C, Peter K. Circ Res. 2006; 99:25–33. [PubMed: 16778135]
12. Esmon CT. Faseb J. 1995; 9:946–955. [PubMed: 7615164]
13. Topcic D, Kim W, Holien JK, Jia F, Armstrong PC, Hohmann JD, Straub A, Krippner G, Haller CA, Domeij H, Hagemeyer CE, Parker MW, Chaikof EL, Peter K. Arterioscler Thromb Vasc Biol. 2011; 31:2015–2023. [PubMed: 21659646]
14. Popp MW, Antos JM, Grotenbreg GM, Spooner E, Ploegh HL. Nat Chem Biol. 2007; 3:707–708. [PubMed: 17891153]
15. Cazalis CS, Haller CA, Sease-Cargo L, Chaikof EL. Bioconjug Chem. 2004; 15:1005–1009. [PubMed: 15366953]
16. Chen I, Dorr BM, Liu DR. Proc Natl Acad Sci U S A. 2011; 108:11399–11404. [PubMed: 21697512]
17. Zhang H, Weingart J, Jiang R, Peng J, Wu Q, Sun XL. Bioconjug Chem. 2013; 24:550–559. [PubMed: 23458546]
18. Garcia-Arevalo C, Bermejo-Martin JF, Rico L, Iglesias V, Martin L, Rodriguez-Cabello JC, Arias FJ. Mol Pharm. 2013; 10:586–597. [PubMed: 23301613]
19. a) Cho EJ, Jung S, Kim HJ, Lee YG, Nam KC, Lee HJ, Bae HJ. Chem Commun (Camb). 2012; 48:886–888. [PubMed: 22139473] b) Matsumoto T, Tanaka T, Kondo A. Langmuir. 2012; 28:3553–3557. [PubMed: 22276782] c) Betancor L, Berne C, Luckarift HR, Spain JC. Chem Commun (Camb). 2006:3640–3642. [PubMed: 17047791] d) Wilner OI, Weizmann Y, Gill R, Lioubashevski O, Freeman R, Willner I. Nat Nanotechnol. 2009; 4:249–254. [PubMed: 19350036]
20. Falati S, Gross P, Merrill-Skoloff G, Furie BC, Furie B. Nat Med. 2002; 8:1175–1181. [PubMed: 12244306]
21. a) Yang J, Hirata T, Croce K, Merrill-Skoloff G, Tchernychev B, Williams E, Flaumenhaft R, Furie BC, Furie B. J Exp Med. 1999; 190:1769–1782. [PubMed: 10601352] b) Proulle V, Furie RA, Merrill-Skoloff G, Furie BC, Furie B. Blood. 2014; 124:611–622. [PubMed: 24825863] c) Jasuja R, Passam FH, Kennedy DR, Kim SH, van Hessem L, Lin L, Bowley SR, Joshi SS, Dilks JR, Furie B, Furie BC, Flaumenhaft R. J Clin Invest. 2012; 122:2104–2113. [PubMed: 22565308]

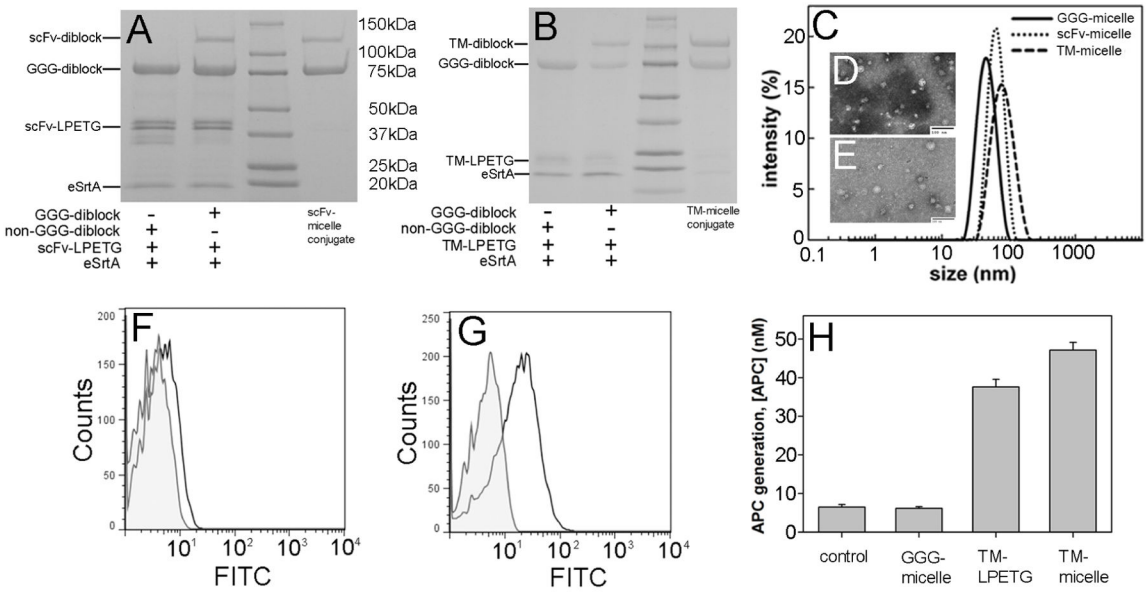

Figure 1. Characterization of protein micelles derivatized with either anti-LIBS-scFv or TM

SDS-PAGE gels showing conjugation of **(A)** scFv and **(B)** TM to protein micelles using sortase. Functionalization of GGG-micelles with therapeutic proteins demonstrates substrate specificity towards the GGG-diblock rather than non-GGG-diblock protein polymers. **(C)** DLS measurements of GGG-micelles (solid), scFv-micelles (dot) and TM-micelles (dash). TEM images of **(D)** scFv-micelles and **(E)** TM-micelles (scale bar: 100 nm). Flow cytometry demonstrates the inability of GGG-micelles **(F)**, but not scFv-micelles **(G)** to bind to activated (white curve) but not resting (gray curve) platelets. **(H)** In vitro aPC generation by TM-micelles and an equivalent amount of TM-LPETG, as a positive control. TM activity was retained after micelle conjugation. GGG-micelles and saline (without TM or GGG-micelles) were used as negative controls (n=3).

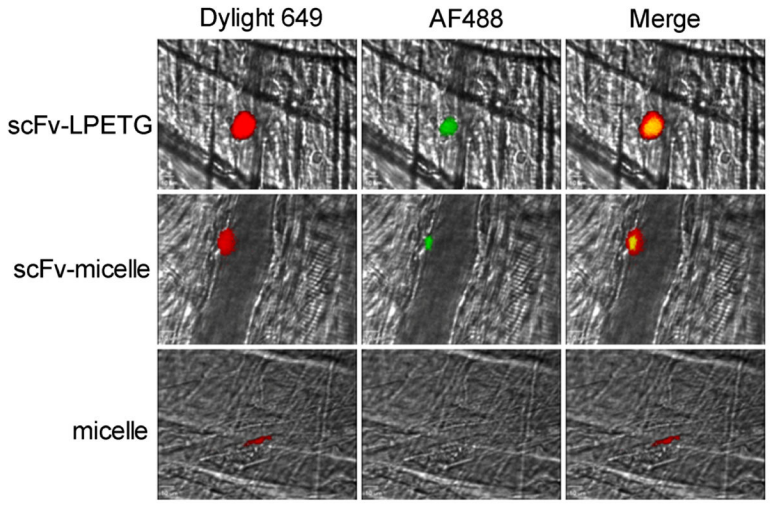

Figure 2. scFv-micelles target to platelet thrombus in vivo

Platelet specific Dylight 649 labeled-anti-CD42b was infused along with either AF488-labeled scFv-LPETG **(top row)**, AF488-labeled scFv-micelles **(middle row)**, or AF488-labeled micelles **(bottom row)** prior to laser injury of cremaster arterioles. Representative images illustrate that scFv-LPETG **(top row)** and scFv-micelles **(middle row)** target to platelet thrombus. Co-localization of non-functionalized GGG-micelles to platelet thrombi was not observed **(bottom row)**.

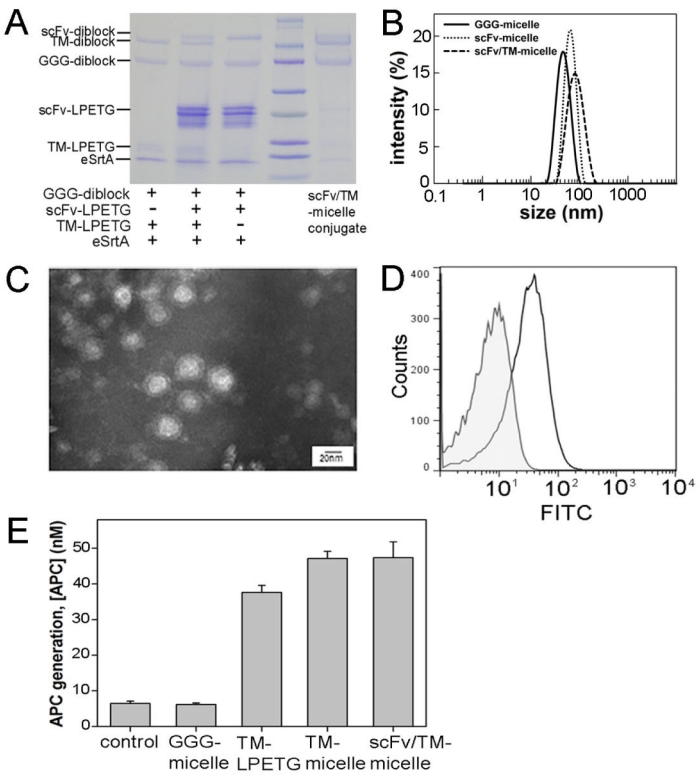

Figure 3. Characterization of protein micelles derivatized with both anti-LIBS-scFv and TM

(A) SDS-PAGE gels demonstrating conjugation of scFv and TM to protein micelles using an evolved sortase. **(B)** DLS measurements of GGG-micelles (solid line), scFv-micelles (dotted line) and scFv/TM-micelles (dashed line). **(C)** TEM images of scFv/TM-micelles (scale bar: 20 nm). **(D)** Flow cytometry assay demonstrating successful conjugation of scFv to protein micelles with specific binding of scFv/TM-micelles to activated (white curve) but not resting platelets (gray curve). **(E)** In vitro aPC generation by scFv/TM-micelles. TM activity was retained after co-functionalization of micelles with both scFv and TM. GGG-micelles and saline (without TM and GGG-micelle) were used as negative controls (n=3).

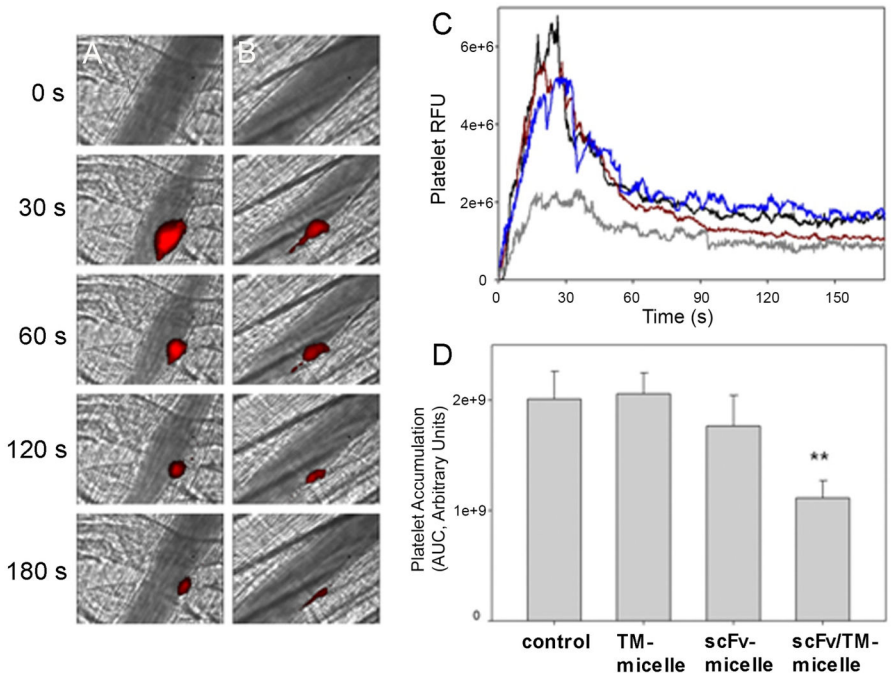

Figure 4. TM-micelles targeted to activated platelets inhibit thrombus formation in vivo

Platelet specific anti-CD42b-Dylight 649 was infused and laser injury induced thrombus formation was characterized over time. Representative images of the fluorescence signal associated with a platelet thrombus after laser injury of cremaster arterioles are administration of **(A)** saline or **(B)** scFv/TM-micelles (0.026 μmol TM/kg). **(C)** Median integrated platelet fluorescence after administration of saline (black), TM-micelles (0.026 μmol TM/kg) (blue), scFv-micelles (red), or scFv/TM-micelles (grey). **(D)** Platelet accumulation was quantified as the area under the curve (AUC) as calculated for platelet RFU. Units are arbitrary and data represents mean ± SEM. A significant reduction in platelet accumulation was observed in those animals treated with scFv/TM-micelles (N=25 thrombi/3 mice/group, $^{**}p < 0.01$)

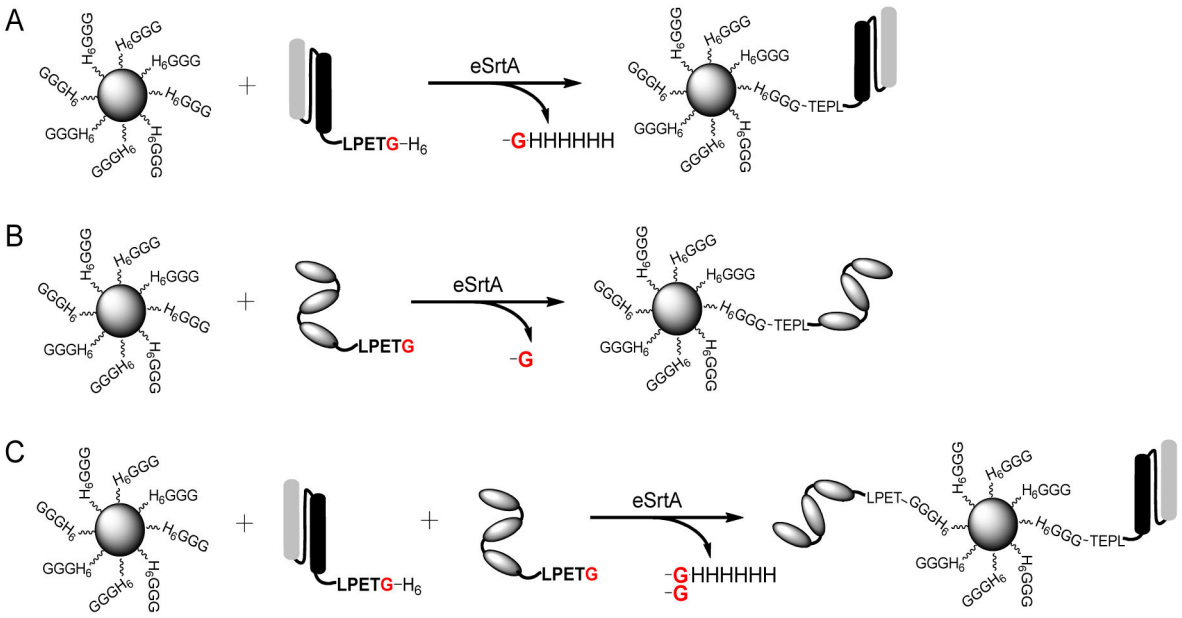

Scheme 1. Preparation of multivalent, multifunctional protein micelles using sortase A
(A) scFv-micelle, **(B)** TM-micelle and **(C)** scFv/TM-micelle.